

Study of CP asymmetry in $B^0\bar{B}^0$ mixing using inclusive dilepton samples

Isabella Garzia on behalf of the *BABAR* Collaboration

INFN-Sezione di Ferrara, via Saragat 1, 44122 Ferrara, Italy

E-mail: garzia@fe.infn.it

Abstract. The asymmetry between same sign inclusive dilepton samples $\ell^+\ell^+$ and $\ell^-\ell^-$ from semileptonic B decays in $\Upsilon(4S) \rightarrow B^0\bar{B}^0$ events allows to compare B mixing probabilities $\mathcal{P}(\bar{B}^0 \rightarrow B^0)$ and $\mathcal{P}(B^0 \rightarrow \bar{B}^0)$, and therefore to test the T and CP invariance. We present the measurement of CP asymmetry in inclusive dilepton samples with the full *BABAR* data set near the $\Upsilon(4S)$ resonance, corresponding to 471 million of $B\bar{B}$ pairs.

1. Introduction

Within the Standard Model (SM), the CP and T symmetries can be violated through weak interaction. For example, a neutral B meson can transform to its antiparticle with a probability $\mathcal{P}(B^0 \rightarrow \bar{B}^0)$ which differs from the probability of oscillation of a \bar{B}^0 into a B^0 : $\mathcal{P}(\bar{B}^0 \rightarrow B^0) \neq \mathcal{P}(B^0 \rightarrow \bar{B}^0)$. This type of CP violation is called CP violation in the mixing, and was observed first in the kaon system [1, 2], but is not been observed in the neutral B system, for which the SM predicts an asymmetry of the order of 10^{-4} [3]. Therefore, a large measured value could be an indication of new physics. The current experimental average of CP asymmetry for the B^0 system is obtained by averaging *BABAR* [4, 5], $D\bar{O}$ [6] and Belle [7] results: $\mathcal{A}_{CP} = (+2.3 \pm 2.6) \times 10^{-3}$. The most recent LHCb result [8], $\mathcal{A}_{CP} = (-0.2 \pm 1.91 \pm 3) \times 10^{-3}$, had not been included in this average. A recent measurement in a mixture of B^0 and B_s^0 meson by the $D\bar{O}$ collaboration [9] deviates from SM prediction by more than three standard deviations, and so the improving of the experimental precision is needed to understand this discrepancy.

The time evolution of the neutral B mesons can be described by an effective Hamiltonian $\mathbf{H} = \mathbf{M} - i\mathbf{\Gamma}/2$, with \mathbf{M} and $\mathbf{\Gamma}$ two Hermitian matrices describing, respectively, the mass and decay-rate components. Assuming CPT symmetry, the light and heavy mass eigenstates can be written as

$$|B_{L/H}\rangle = p|B^0\rangle \pm q|\bar{B}^0\rangle, \quad (1)$$

where p and q are complex mixing parameters normalized to $|p|^2 + |q|^2 = 1$. If $|q/p| \neq 1$, both CP and T asymmetries are violated. The B -factories operate at the center-of-mass (c.m.) of the $\Upsilon(4S)$ resonance, which decays into a $B^0\bar{B}^0$ pair about 50% of times. This pair evolves coherently until one B meson decays. In particular, in this analysis, we identify the flavor of one of the B meson at the time of its decay by looking the charge of the lepton (electron or muon) produced from its semileptonic decay. If the second B meson has oscillated, it will produce a lepton with the same charge as the lepton from the first B decay. The CP asymmetry between



$\mathcal{P}(\bar{B}^0 \rightarrow B^0)$ and $\mathcal{P}(B^0 \rightarrow \bar{B}^0)$ is obtained by measuring the charge asymmetry of the same-sign dilepton event rates $\mathcal{P}_{\ell\ell}^{\pm\pm}$

$$\mathcal{A}_{CP} = \frac{\mathcal{P}_{\ell\ell}^{++} - \mathcal{P}_{\ell\ell}^{--}}{\mathcal{P}_{\ell\ell}^{++} + \mathcal{P}_{\ell\ell}^{--}} = \frac{1 - |q/p|^4}{1 + |q/p|^4}, \quad (2)$$

which is a quantity independent of the B decay time.

In this analysis, we present an update of \mathcal{A}_{CP} using inclusive dilepton events [10] collected by the *BABAR* detector. In contrast to the previous *BABAR* dilepton analysis [4], we use a new strategy based on a counting procedure, which does not require the proper decay time difference distribution Δt of the two B mesons.

2. The *BABAR* detector and data sample

The *BABAR* detector is described in detail in Ref. [11], so here we give only a brief description of the apparatus. Surrounding the beam-pipe, there is a five-layer silicon vertex detector (SVT), which gives very precise measurements of the vertex decays. Outside the SVT there is a 40-layer drift chamber (DCH) filled with a helium-isobutane (80:20) gas mixture. The DCH and SVT measurements of dE/dx energy loss also contributes to the charged particle identification (PID). After the DCH, there is the detector of internally reflected Cerenkov radiation (DIRC), which gives charged-particle identification. Outside the DIRC, an highly segmented electromagnetic calorimeter (EMC), composed of CsI(Tl) crystals, is used to detect photons and electrons. Finally, the flux return of the superconducting coil surrounding the EMC is instrumented with resistive plate chambers or limited streamer tubes interleaved with iron for the identification of muons and neutral hadrons.

The data set used for this analysis consists of 471×10^6 $B\bar{B}$ pairs produced at the c.m. energy of the $\Upsilon(4S)$ resonance (on-peak data sample), collected by the *BABAR* detector at the PEP-II asymmetric-energy e^+e^- storage ring at the SLAC National Accelerator Laboratory. A smaller sample, about 44 fb^{-1} , of data is collected 40 MeV below the $\Upsilon(4S)$ (off-peak sample), and is used to study background from $e^+e^- \rightarrow q\bar{q}$ events (continuum background). The analysis procedure is tested on a Monte Carlo (MC) simulated $B\bar{B}$ event sample.

3. Analysis strategy

We select an event if the two particles with highest momentum are consistent with electron or muon hypothesis. In not otherwise specified, all quantities are evaluated in the c.m. frame. We construct the following four leptons combinations: $\ell_1\ell_2 = ee, e\mu, \mu e, \mu\mu$, where ℓ_1 (ℓ_2) refers to the highest- (lower-) momentum lepton candidate. Taking into account the four charge combination, we have a total of 16 subsamples. For events originating from two semileptonic B decays, the time-integrated signal yields for same-sign $N_{\ell_1\ell_2}^{\pm\pm}$ (mixed) and opposite-sign $N_{\ell_1\ell_2}^{\pm\mp}$ (unmixed) lepton pairs can be written as

$$N_{\ell_1\ell_2}^{\pm\pm} = \frac{1}{2} N_{\ell_1\ell_2}^0 (1 \pm a_{\ell_1})(1 \pm a_{\ell_2})(1 \pm \mathcal{A}_{CP}) \chi_d^{\ell_1\ell_2} \quad (3)$$

$$N_{\ell_1\ell_2}^{\pm\mp} = \frac{1}{2} N_{\ell_1\ell_2}^0 (1 \pm a_{\ell_1})(1 \mp a_{\ell_2})(1 - \chi_d^{\ell_1\ell_2} + r_B), \quad (4)$$

where $N_{\ell_1\ell_2}^0$ is the total time-integrated $B^0\bar{B}^0$ dilepton yield for the $\ell_1\ell_2$ lepton flavor combination, $a_{\ell_j} = (\epsilon_{\ell_j}^+ - \epsilon_{\ell_j}^-)/(\epsilon_{\ell_j}^+ + \epsilon_{\ell_j}^-)$ is the charge asymmetry of the detection efficiency for lepton j , $\chi_d^{\ell_1\ell_2}$ is the effective mixing probability of neutral B mesons including efficiency corrections, and r_B represents the ratio of total B^+B^- yield to the total $B^0\bar{B}^0$ yield.

The number of events observed in the data can be obtained by dividing the total time-integrated yields by the signal fractions $f_{\ell_1\ell_2}$. The signal fraction for same-sign leptons can be

written as

$$f_{\ell_1\ell_2}^{\pm\pm} = \frac{S_{\ell_1\ell_2}^{\pm\pm}(1 \pm \mathcal{A}_{CP})}{S_{\ell_1\ell_2}^{\pm\pm}(1 \pm \mathcal{A}_{CP}) + B_{\ell_1\ell_2}^{\pm\pm}} = \frac{1 \pm \mathcal{A}_{CP}}{1 \pm \mathcal{A}_{CP} + B_{\ell_1\ell_2}^{\pm\pm}/S_{\ell_1\ell_2}^{\pm\pm}}, \quad (5)$$

where S and B are the signal and background. Note that, since the signal is generated without CP asymmetry, we need to correct the simulated same-sign signal by a factor $1 \pm \mathcal{A}_{CP}$.

The same-sign background is dominated by unmixed events with a cascade lepton from $B \rightarrow X \rightarrow \ell Y$ decay, which does not have CP asymmetry. However, a small fraction of same-sign background events originate from mixed events. Some of this mixed events have the B flavor consistent with the measured charge of the lepton pairs, and other events have the opposite B flavor with respect to the measured charge of the lepton pairs. This two types of events could have an opposite effect due to a non-zero \mathcal{A}_{CP} . We calculate the dilution factor $\delta_{\ell_1\ell_2}$, defined as the probability of a same-sign background event being consistent with the flavor of the neutral B pairs at the time of their decay after the mixing, i.e. $\ell^+\ell^+$ for B^0B^0 or $\ell^-\ell^-$ for $\bar{B}^0\bar{B}^0$, minus the probability of the opposite case, i.e. $\ell^+\ell^+$ for $\bar{B}^0\bar{B}^0$ or $\ell^-\ell^-$ for B^0B^0 . Using this dilution factor, the background events $B_{\ell_1\ell_2}^{\pm\pm}$ in Eq. (5) became $(1 \pm \delta_{\ell_1\ell_2}\mathcal{A}_{CP})B_{\ell_1\ell_2}^{\pm\pm}$.

In the limit of $\mathcal{A}_{CP} \ll 1$ and $a_{\ell_1(\ell_2)} \ll 1$, the number of events observed in the data are

$$M_{\ell_1\ell_2}^{\pm\pm} = \frac{N_{\ell_1\ell_2}^{\pm\pm}}{f_{\ell_1\ell_2}^{\pm\pm}} = \frac{1}{2}N_{\ell_1\ell_2}^0(1 + R_{\ell_1\ell_2}^{\pm\pm}) \left[1 \pm a_{\ell_1} \pm a_{\ell_2} \pm \frac{1 + \delta_{\ell_1\ell_2}R_{\ell_1\ell_2}^{\pm\pm}}{1 + R_{\ell_1\ell_2}^{\pm\pm}}\mathcal{A}_{CP} \right] \chi_d^{\ell_1\ell_2}, \quad (6)$$

where $R_{\ell_1\ell_2}^{\pm\pm} = B_{\ell_1\ell_2}^{\pm\pm}/S_{\ell_1\ell_2}^{\pm\pm}$.

For opposite-sign events, the signal comes from unmixed events and, therefore, it is CP symmetric. A small fraction of background comes from mixed events, but its contribution can be neglected in the final fit. In the limit of $\mathcal{A}_{CP} \ll 1$ and $a_{\ell_1(\ell_2)} \ll 1$, the number of opposite-sign events can be written as:

$$M_{\ell_1\ell_2}^{\pm\mp} = \frac{N_{\ell_1\ell_2}^{\pm\mp}}{f_{\ell_1\ell_2}^{\pm\mp}} = \frac{1}{2}N_{\ell_1\ell_2}^0(1 + R_{\ell_1\ell_2}^{\pm\mp})(1 \pm a_{\ell_1} \mp a_{\ell_2}) \left(1 - \chi_d^{\ell_1\ell_2} + r_B \right). \quad (7)$$

We build a χ^2 fit using the 16 observables so measured. There are thirteen unknowns parameters, \mathcal{A}_{CP} , $\chi_d^{\ell_1\ell_2}$, $a_{\ell_1(\ell_2)}$, $N_{\ell_1\ell_2}^0$, and in principle it is possible to fit them at once. However, the strong correlation between the CP asymmetry and the charge asymmetry of lepton detection efficiency produces a very large uncertainties.

We overcome this problem adding another term in the χ^2 fit in order to constrain the detector efficiency $a_\ell \equiv (a_{\ell_1} + a_{\ell_2})/2$. We use single-lepton events (number of lepton ≥ 1) and we measure the asymmetry a_{on} in the on-peak data sample, which is determined mostly by the detection efficiency with a small dependence on \mathcal{A}_{CP} . It can be expressed as

$$a_{on} = \alpha + \beta\chi_d\mathcal{A}_{CP} + \gamma a_\ell, \quad (8)$$

where the α , β , and γ parameters are expressed as a combination of several variables that can be extracted from single lepton data sample, data control sample, and MC sample.

We include Eq. (8) in the χ^2 fit to extract \mathcal{A}_{CP} .

4. Event selection

We select events with at least 4 charged tracks and with the normalized second-order Fox-Wolfram momentum [12] $R_2 < 0.6$. We use leptons with momentum $0.6 \text{ GeV} < p_\ell < 2.2 \text{ GeV}$ and with the polar angle θ in the laboratory frame $-0.788 < \cos\theta < 0.961$ for electron and $-0.755 < \cos\theta < 0.956$ for muon candidates. The lepton is rejected if, when combined with

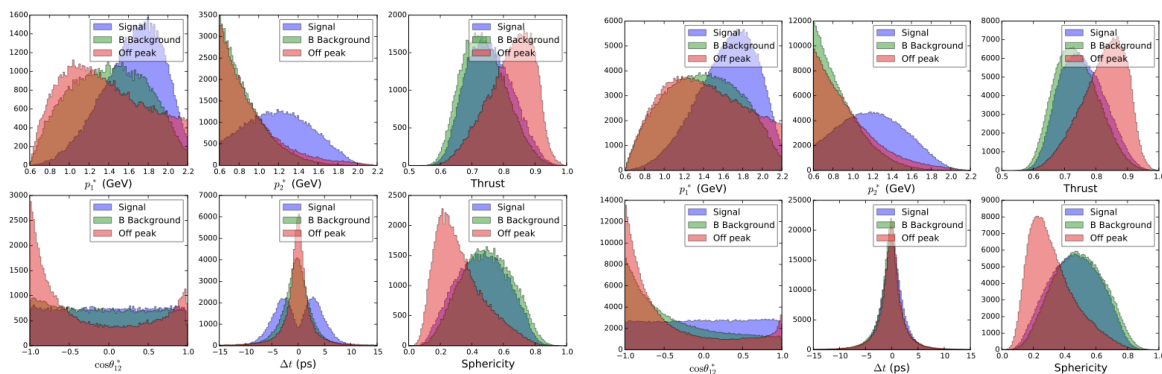


Figure 1. Kinematical variable distributions in same-sign (left) and opposite-sign sample (right).

another lepton of opposite charge, the invariant mass is consistent with the J/ψ or a $\psi(2S)$ meson, or when it arises from a photon conversion.

For dilepton events, the invariant mass of the lepton pairs must be greater than 150 MeV. We require $\Delta t < 15$ ps and its uncertainties $\sigma_{\Delta t} < 3$ ps, where Δt is the proper decay time difference of the two B mesons.

Electrons and muons are identified by two separate multivariate algorithms. The algorithm for electrons is based mainly on the shower shape and the energy deposition in the EMC, while that one for muons uses the track path length and cluster shape in the instrumented flux return. The electron identification efficiency is about 93%, while it ranges from 40% to 80% for muons as a function of the momentum. The probability of a hadron being identified as an electron or muon is less than 0.1% and around 1%, respectively.

5. Background suppression

The main sources of background are continuum events and cascade leptons from $B\bar{B}$ events. The continuum contribution is studied using off-peak data, while a Random Forest multivariate classifier [13] is used to suppress $B\bar{B}$ background.

In the dilepton sample, we use six variables: the c.m. momenta of the two tracks ($p_{1,2}^*$), the thrust and sphericity of the rest of the event, the opening angle of the two tracks (θ_{12}^*) in the c.m. frame, and Δt . The distributions for the same-sign and opposite-sign samples are shown in Fig. 1. The four lepton sample combinations are trained separately, as well as the same sign and opposite sign samples, and Fig. 2 shows the signal probability distributions of the classifiers. We select events with a probability > 0.7 in order to minimize the statistical uncertainty. After this selection, about 2.5% of events come from continuum background, and 35% (8%) from $B\bar{B}$ background in same-sign (opposite-sign) sample.

For the single-lepton sample, we train the Random Forest classifier in order to suppress the continuum background. We use the number of tracks, the event thrust, the R_2 distribution, the difference between the observed energy in the event and the sum of beam energy, the cosine of the angles between the lepton and the axes of the thrust and the sphericity of the rest of the event, and the zeroth-order and second-order polynomial moments L_0 and L_2 , where $L_n = \sum_i p_i (\cos \theta_i)^n$, p_i is the momentum of the track in the rest of the event and θ_i is the angle between this track and the single-lepton candidate. We optimize the selection requirement by minimizing the uncertainty of the charge asymmetry after the continuum background subtraction from the on-peak data sample. We found that about 63% of the selected single electrons come from direct semileptonic B decays.

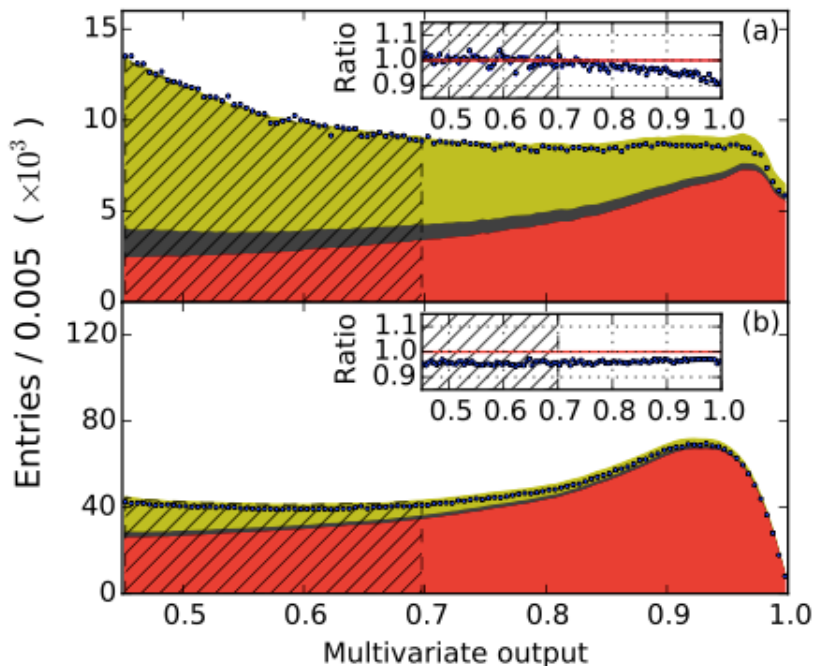


Figure 2. Signal probability distributions from the dilepton multivariate algorithm for (a) same-sign sample and (b) opposite-sign sample. Points represent the continuum-subtracted data, shaded regions from bottom to top indicate the signal, $B\bar{B}$ background with at least one misidentified lepton, and $B\bar{B}$ background with both real leptons. In the inset plots are shown the data/MC ratio. Hatched region is rejected.

5.1. Fake lepton component

In the $B\bar{B}$ background we can distinguish two different components. The first is when both leptons are correctly identified. In this case, the background-to-signal ratio does not depend on the charge asymmetry of the particle identification (PID), because it is cancelled out. The second component originates from the misidentification of at least one lepton, and is called fake lepton background. In this case, the background-to-signal ratio fully depends on the misidentification efficiency.

Approximatively, 3% (0.1%) of the selected muons (electrons) in the dilepton sample are misidentified. From MC simulation, we found that about 98% of mis-identified electrons come from pions, while 87% (12%) of misidentified muons come from pions (kaons). To correct for the difference in the muon misidentification rates between data and MC, we study the muon misidentification efficiency using a clean kaon and muon control samples ($D^* \rightarrow D^0\pi^+$, $D^0 \rightarrow K^-\pi^+$). The ratio of the efficiencies between data and MC are used to scale the misidentification component in the MC sample. Due to the very low misidentification rate for electrons, a much larger pions control sample from $K_s \rightarrow \pi^+\pi^-$ decays is used.

6. Asymmetry results and χ^2 fit

The measurement of the raw asymmetries of the single electrons is $a_{on} = (4.12 \pm 0.14) \times 10^{-3}$ in the on-peak sample, and $a_{off} = (11.1 \pm 1.4) \times 10^{-3}$ in the off-peak data sample. The larger asymmetries observed in the off-peak data is primarily due to the radiative Bhabha events and to the large forward/backward asymmetry of the *BABAR* detector. We determine the numerical

value of the coefficients in Eq. (8): $a_{on} - \alpha = (2.60 \pm 0.20) \times 10^{-3}$, $\beta\chi_d = 0.057 \pm 0.001$, and $\gamma = 0.8951 \pm 0.0002$.

\mathcal{A}_{CP} is obtained from a χ^2 fit to the 16 continuum-subtracted yields (Eqs. (6), (7)), reported in Table. 1, plus the constraint of Eq. (8).

Table 1. Continuum-subtracted event yields.

	$\ell^+\ell^+$	$\ell^+\ell^-$	$\ell^-\ell^+$	$\ell^-\ell^-$
ee	82303 ± 320	426296 ± 783	425309 ± 782	81586 ± 323
$e\mu$	55277 ± 263	384552 ± 684	378261 ± 660	55878 ± 264
μe	67399 ± 290	467591 ± 737	475363 ± 744	67152 ± 290
$\mu\mu$	47384 ± 243	277936 ± 691	278691 ± 618	48145 ± 247

The fitting procedure is tested on the $B\bar{B}$ MC sample. We measure $\mathcal{A}_{CP}^{MC} = (-1.00 \pm 1.04) \times 10^{-3}$, in agreement with the expectation of no CP asymmetry. In addition, we simulate a non-zero value of asymmetry by reweighing mixed events in the MC sample. We found that the fitting procedure is able to reproduce the asymmetry without bias.

The \mathcal{A}_{CP} measure, after the correction for the small MC bias, is reported in Table 2, where are also summarized all the other parameters extracted from the fit.

Table 2. Parameters of the nominal χ^2 fit. The value of \mathcal{A}_{CP} is corrected for the small MC bias of -1×10^{-3} . Only statistical errors are reported.

$\mathcal{A}_{CP} = (-3.9 \pm 3.5) \times 10^{-3}$				
	ee	$e\mu$	μe	$\mu\mu$
N^0	430875 ± 515	365343 ± 428	458200 ± 480	268077 ± 391
χ_d	0.2248 ± 0.0006	0.1769 ± 0.0006	0.1754 ± 0.0005	0.2032 ± 0.0007
	a_{e_1}	a_{e_2}	a_{μ_1}	a_{μ_2}
a	0.0034 ± 0.0006	0.0030 ± 0.0006	-0.0056 ± 0.0011	-0.0065 ± 0.0011

7. Systematic uncertainties

Several sources of systematic uncertainties are taken into account, and in this section we report those that are significant. The final systematic uncertainty on \mathcal{A}_{CP} is the sum in quadrature of these effects.

Generic MC test. The generic MC is generated with $\mathcal{A}_{CP} = 0$. The fit result is $\mathcal{A}_{CP}^{MC} = (-1.00 \pm 1.04) \times 10^{-3}$, which is consistent with zero. We correct \mathcal{A}_{CP} for this bias and we assign the statistical error as systematic contribution.

MC branching fractions. The branching fractions in B decay chains influence the determination of the background-to-signal ratio, and thus affect \mathcal{A}_{CP} . We vary the inclusive charm and semileptonic branching fractions by taking into account the difference between the values reported in PDG [14] and those used by EvtGen in the simulation. The result of \mathcal{A}_{CP} is shifted by $+0.43 \times 10^{-3}$. We take this value as systematic contributions.

Misidentified lepton corrections. We vary the efficiency corrections of leptons within their uncertainties. The systematic contribution is determined by the change in \mathcal{A}_{CP} , and is equal to 0.77×10^{-3} . The fake electron asymmetry and fraction also affect \mathcal{A}_{CP} through Eq. (8). The fake fraction is estimated using MC sample and then it is corrected by the data to MC efficiency ratio. By varying this ratio in the single lepton analysis, we found a variation of 0.53×10^{-3} in the measure of \mathcal{A}_{CP} , which is taken as systematic uncertainty.

Discrepancy between neutral and charged B mesons. In the single-electron MC sample, the difference between the charge asymmetry of the direct electron in $B^0\bar{B}^0$ and B^+B^- sample is $(0.46 \pm 0.18) \times 10^{-3}$. Since in real data we cannot distinguish neutral and charged B mesons, the single-electron asymmetry measurement is the average of the two asymmetries. We calculate \mathcal{A}_{CP} after shifting the asymmetry in the signal component of the single-electron sample by half of the charge asymmetry difference. The change in \mathcal{A}_{CP} is taken as systematic uncertainty.

Direct/cascade e and μ asymmetry difference. The asymmetry difference between cascade and direct electron (muon) in MC is $\delta_e^{casc} = (-1.16 \pm 0.25) \times 10^{-3}$ ($\delta_\mu^{casc} = (-0.47 \pm 0.28) \times 10^{-3}$). The difference is due to the fact that the charge asymmetry depends on the lepton kinematics. The same trend is observed in the fit results of the dilepton data sample: the asymmetry difference between the lower-momentum and the higher-momentum lepton is negative. We change the asymmetry in the cascade electron (muon) component by the δ_e^{casc} (δ_μ^{casc}) amount, and we take the difference in \mathcal{A}_{CP} , -0.44×10^{-3} (-0.34×10^{-3}), as systematic uncertainty.

Background-to-signal ratios. The background-to-signal ratio $R_{\ell_1\ell_2}^{\pm\pm(\pm\mp)}$ are obtained from simulation under the condition of $\mathcal{A}_{CP} = 0$. If we vary simultaneously and in the same direction $R_{\ell_1\ell_2}^{++}$ and $R_{\ell_1\ell_2}^{--}$, as well as $R_{\ell_1\ell_2}^{+-}$ and $R_{\ell_1\ell_2}^{-+}$, we found a negligible change in the \mathcal{A}_{CP} value. If they are varied independently, the quadratic sum of the variation in \mathcal{A}_{CP} is 0.68×10^{-3} , which is taken as systematic uncertainty.

Efficiency in random forest cut. The random forest selection efficiency is about 2.6% larger in MC than in data sample for the same-sign events. We vary the random forest selection for MC in order to reduce the selected MC events. The average change in \mathcal{A}_{CP} (0.08×10^{-3}) is taken as systematic uncertainty.

8. Summary and conclusions

We study the CP asymmetry in $B^0\bar{B}^0$ mixing for inclusive dilepton decays using the full *BABAR* data set [10]. We measure $\mathcal{A}_{CP} = (-3.9 \pm 3.5 \pm 1.9) \times 10^{-3}$, where the error are statistical and systematic, respectively. The comparison with the current experimental results and averages are shown in Fig. 3. This result is consistent with the SM prediction, the world average [15], and with the recent LHCb measure [8], and represent a significant improvement with respect to our previous results [4], as well as is one of the most precise measurements.

References

- [1] Christenson J H, Cronin J W, Fitch V L and Turlay R 1964 *Phys. Rev. Lett.* **13**(4) 138–140
- [2] Dorfan D, Enstrom J, Raymond D, Schwartz M, Wojcicki S, Miller D H and Paciotti M 1967 *Phys. Rev. Lett.* **19**(17) 987–993
- [3] Lenz A, Nierste U, Charles J, Descotes-Genon S, Jantsch A, Kaufhold C, Lacker H, Monteil S, Niess V and T’Jampens S 2011 *Phys. Rev. D* **83**(3) 036004
- [4] Aubert B *et al.* 2006 *Phys. Rev. Lett.* **96**(25) 251802
- [5] Lees J P *et al.* 2013 *Phys. Rev. Lett.* **111**(10) 101802
- [6] Abazov V M *et al.* 2012 *Phys. Rev. D* **86**(7) 072009

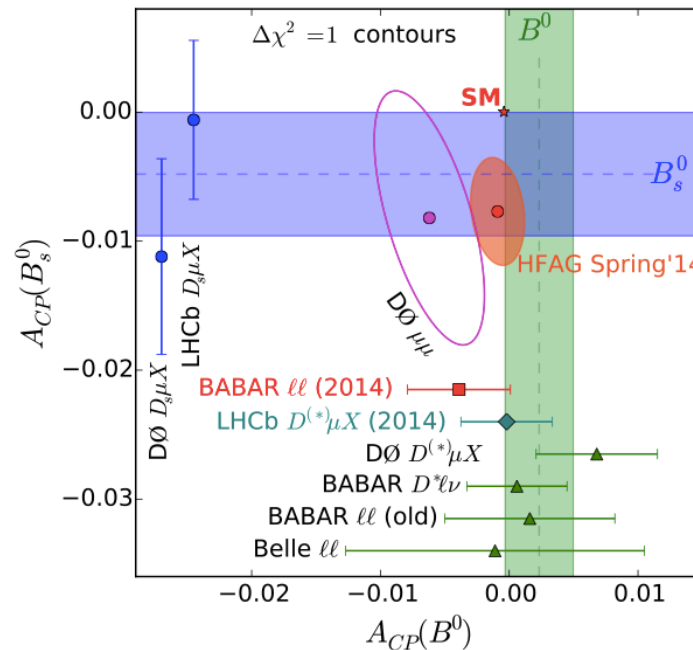


Figure 3. Measurement of CP asymmetry in neutral B mixing. The red square represent this measurement, teal rhombus the recent LHCb result [8], green triangles the B^0 results from Refs. [4, 5, 6, 7] with the vertical band their average, blue circles the B_s^0 results from Refs. [16, 17] with the horizontal band their average, and the magenta point and contour indicate the B^0 - B_s^0 mixture from Ref. [9]. The word average "HFAG Spring '14" [15] is also shown by the orange region.

- [7] Nakano E *et al.* 2006 *Phys. Rev. D* **73**(11) 112002
- [8] Aaij R *et al.* ((LHCb Collaboration)) 2015 *Phys. Rev. Lett.* **114**(4) 041601
- [9] Abazov V M and Others ((D0 Collaboration)) 2014 *Phys. Rev. D* **89**(1) 012002
- [10] Lees J P *et al.* ((BABAR Collaboration)) 2015 *Phys. Rev. Lett.* **114**(8) 081801
- [11] Aubert B *et al.* 2013 *Nuclear Instruments and Methods in Physics Research Section A: Accelerators, Spectrometers, Detectors and Associated Equipment* **729** 615 – 701 ISSN 0168-9002
- [12] Fox G C and Wolfram S 1978 *Phys. Rev. Lett.* **41**(23) 1581–1585
- [13] Pedregosa F, Varoquaux G, Gramfort A, Michel V, Thirion B, Grisel O, Blondel M, Prettenhofer P, Weiss R, Dubourg V, Vanderplas J, Passos A, Cournapeau D, Brucher M, Perrot M and Duchesnay E 2011 *Journal of Machine Learning Research* **12** 2825–2830
- [14] Olive K *et al.* (Particle Data Group) 2014 *Chin. Phys.* **C38** 090001
- [15] Y. Amhis *et al.* (Heavy Flavor Averaging Group) (2012), arXiv:1207.1158 and online update <http://www.slac.stanford.edu/xorg/hfag/osc/spring.2014/> accessed: 2010-09-30
- [16] Abazov V M *et al.* ((D0 Collaboration)) 2013 *Phys. Rev. Lett.* **110**(1) 011801
- [17] 2014 *Physics Letters B* **728** 607 – 615 ISSN 0370-2693